IJNRD.ORG ISSN : 2456-4184
INTERNATIONAL JOURNAL OF NOVEL RESEARCH AND DEVELOPMENT (IJNRD) | IJNRD.ORG
An International Open Access, Peer-reviewed, Refereed Journal

Gold Nanoparticle: Fastest Tool for Onsite Monitoring of Pesticides

Anand Besekar*[1, 2], Rasleen Kaur[1], Priya Katiyar[1], Anita Bhoi[1], Lakshita Dewangan[2], Manmohan L Satnami[2] and S Keshavkant[1]

[1]School of Studies in Biotechnology, Pt. Ravishankar Shukla University, Raipur 492 010, Chhattisgarh, India

[2]School of Studies in Chemistry, Pt. Ravishankar Shukla University, Raipur 492 010, Chhattisgarh, India

Abstract

Chemical pesticides are the large heterogeneous compounds which are employed in the modern agriculture. Paraoxon belongs to the class of organophosphate pesticides which has been used extensively in the agricultural fields. The overuse of pesticides results in the harmful impact over the ecological system and human health. Paraoxon is a non-degradable pesticide but can be transformed in the environment by hydrolysis/ photolysis thereby producing severely harmful chemicals. The paraoxon is noticeably recognized to inactivate the catalytic activity of the enzyme acetylcholinesterase. Nanoparticles (NPs) of various metals are largely reported to be loaded with enormous typical properties and a good stability. In line, gold NPs (AuNPs) are one of the most stable NPs that can been prepared following various techniques in different shapes and structures. These have been displayed best applicability in various aspects owing to their simple preparation, stability, smooth functionalization and remarkable color modifications. The red color of the well-dispersed AuNPs changes into blue coloration upon aggregation. Based on this, AuNPs have been effectively utilized for the detection of many pollutants present in the environment. In the present study, a change in the color of the AuNPs from red to slight black have been observed in presence of paraoxon, and was triggered by the addition of sodium chloride. The technique evolved is quite simple and does not require any expensive chemicals or instruments. The change in color was very rapid and was observed by the bare eye. Thus, this colorimetric technique may probably be utilized for onsite monitoring of pesticides.

Graphical abstract

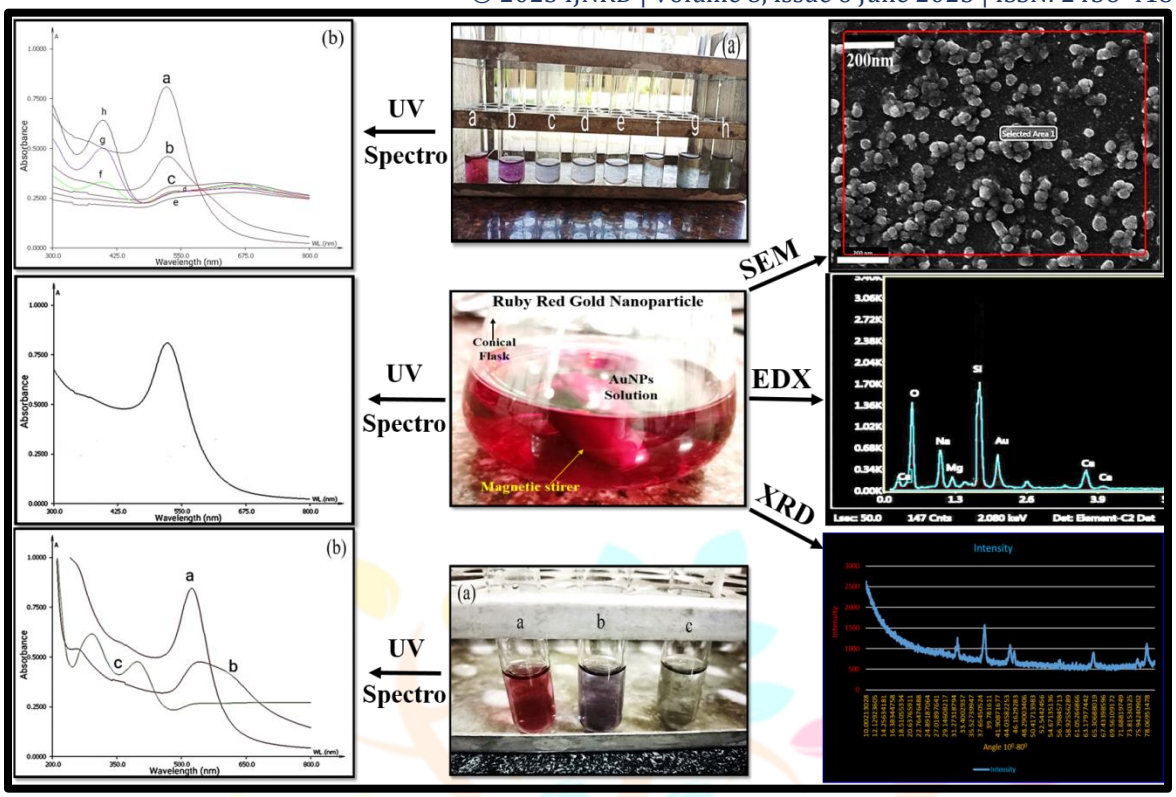

Key words: Gold Nanoparticle, Nanoparticle, Organophosphate, Paraoxon, Pesticide

1. Introduction

Nanomaterials are tiny materials in which at least one dimension of the three-dimensional space is at the nanometer scale (1nm-100 nm) [1, 2]. Nanoparticles (NPs) are an example of nanomaterials loaded with enormous applicability. Nanoparticles play an important role in various fields such as biology, physics, chemistry, medicine and sensing, *etc*., due to their unique properties [3, 4]. Gold NPs (AuNPs) are the most stable NPs and can been prepared by various techniques in different shapes and structures including nanospheres, nanorods, nanocubes, nanobranches, *etc*. [5, 6, 7, 8].

The very initial work on NPs was done by Faraday in 1857. He reported the light scattering potential of NPs and was confirmed it by the colloidal nature and change in color of nanomaterials [9]. For the synthesis of NPs of precise and stable structure there are two distinct methods called as top-down and bottom-up.

The top-down method begins with the wounding of bulk materials and ending with self-assembled nanoscale objects [10]. Photolithography and micropatterning are the two most mutual methods in top-down process [11, 12]. The bottom-up method is widely used technique in recent years. Synthesis of NPs can be done by three methods that are physical, chemical and biological. The chemical reduction of metal ions in solutions is done through introducing reducing and stabilizing agents, for example; sodium borohydride ($NaBH_4$), tri-sodium citrate ($Na_3C_6H_5O_7$), *etc*. Citrate stabilized AuNPs (here after referred as AuNPs) were firstly synthesized by Turkevich et al. in 1951 [13], which was the first chemical synthesis of these NPs. This synthesis was done through the single step aqueous

reduction of $HAuCl_4$ by sodium citrate. This synthesis was further modified by Frens in 1973 by changing the ratio of sodium citrate and Au salt in order to control the size of AuNPs from 5 to 150 nm [14].

Various analytical strategies had been developed to characterize NPs of noble metals with their specific thermal, electrical, chemical and optical properties and to confirm their size, shape, distribution, surface morphology, surface charge, and surface area [15, 16, 10].

Chemical pesticides are the large heterogeneous compounds which are heavily employed in modern agriculture. In terms of their chemical structures, pesticides can be classified into four leading groups including organochlorines, organophosphate (OP), carbamate, chlorophenols and synthetic pyrethroids. These are used for protecting crops, controlling insects, pests and improving productivity [17,18]. On the basis of their function, they may be classified into five groups that consists of insecticides, herbicides, fungicides, rodenticides and nematocides [19, 20, 21]. Many pesticides have been notably utilized in agriculture because of their low price and excessive effectiveness. The overuse of insecticides results in the harmful impact over the ecological system and human health [22, 23]. Additionally, some of the pesticides causes endocrine disruption and have been concerned with neurotoxicity, genotoxicity, mutagenicity and carcinogens. Among various classes of pesticides, OP poisoning has been a major cause of concern in the world, due to its severe effects on the nervous and reproductive systems of living beings [24, 25, 26].

Paraoxon belongs to the class of OP pesticides which has been seen to be used extensively in the agricultural fields. Paraoxon is naturally found in *Apis cerana indica* and it can also be prepared chemically. Chemical formula of paraoxon is $C_{10}H_{14}NO_6P$ and its molecular weight is 275.19. It is characterized as a reddish-yellow oily liquid with a faint fruity odor. Its exposure occurs by inhalation, ingestion and contact. It is a non-degradable pesticide but can be transform in the environment by hydrolysis and photolysis forming exclusive harmful chemicals which affects human health severely.

The paraoxon is noticeably recognized to inactivate the catalytic activity of the enzyme acetylcholinesterase (AChE) which is a crucial component involved in the cholinergic functions in the central and peripheral nervous systems. Inhibition of the activity of acetylcholine causes serious complications like nausea, dizziness, confusion and its excessive exposure lead to respiratory diseases, paralysis and death. It is suspected to cause kidney problems, birth defects and child leukemia. However, the growing utilization of paraoxon has posed a critical situation in the surrounding along with human being and different living organisms [27].

Water pollution due to the excessive use of pesticides is a vital problem in developing countries. It is urgent to develop sensitive, selective and low-cost analytical strategies to reveal the presence of pesticides in real-world samples.

Gold NPs were effectively utilized for the detection of many pollutants present in the environment. The AuNPs in particular, have displayed best results owing to their simple preparation, excessive extinction coefficient, more stability, smooth functionalization and remarkable color modifications. The red color of the well-dispersed AuNPs

changes into blue coloration upon aggregation, ensuring shifting of the surface plasmon band to an extended wavelength, a characteristic that is hired extensively in optical sensing of pollutants.

Here, we have employed the color change of AuNPs from red to blue, and from blue to slightly black by salt triggered aggregation procedure for the detection of presence/ absence of a common pesticide paraoxon. The technique evolved will be quite simple and not require any expensive chemicals. The reaction was very rapid and observed by the bare eye. It is not demanding any laborious sample preparation and may be done through inexperienced hands. This colorimetric technique may probably be utilized for onsite monitoring of pesticides.

2. Materials and Methods

2.1 Materials Required

Millipore Milli-Q (Millipore, Merck, USA) water was used in all the experiments. Hydrogen tetrachloroaurate trihydrate ($HAuCl_4 \cdot 3H_2O$), tri-sodium citrate ($Na_3C_6H_5O_7$), sodium borohyride ($NaBH_4$), sodium chloride (NaCl), potassium chloride (KCl), potassium di-hydrogen phosphate (KH_2PO_4), di-sodium hydrogen phosphate (Na_2HPO_4) and paraoxon ($C_{10}H_{14}NO_6P$) used were of analytical grades (HiMedia, India).

2.2 Methods:

2.2.1 Synthesis of AuNPs

Gold NPs were synthesized by the reduction of hydrogen tetrachloroauratetrihydrate ($HAuCl_4.3H_2O$) with trisodium citrate ($Na_3C_6H_5O_7$) which served as a capping agent. Sodium borohydride ($NaBH_4$) acted as a reducing agent for the conversion of bulk material of Au salt into nanoscale dimension. The 0.13 mM $HAuCl_4.3H_2O$ was diluted with 50 mL of Milli-Q water with continuous stirring over a magnetic stirrer. Thereafter, 0.1 M tri-sodium citrate solution was added to this suspension followed by drop wise addition of 0.1 M sodium borohydride until the solution turns ruby red in appearance.

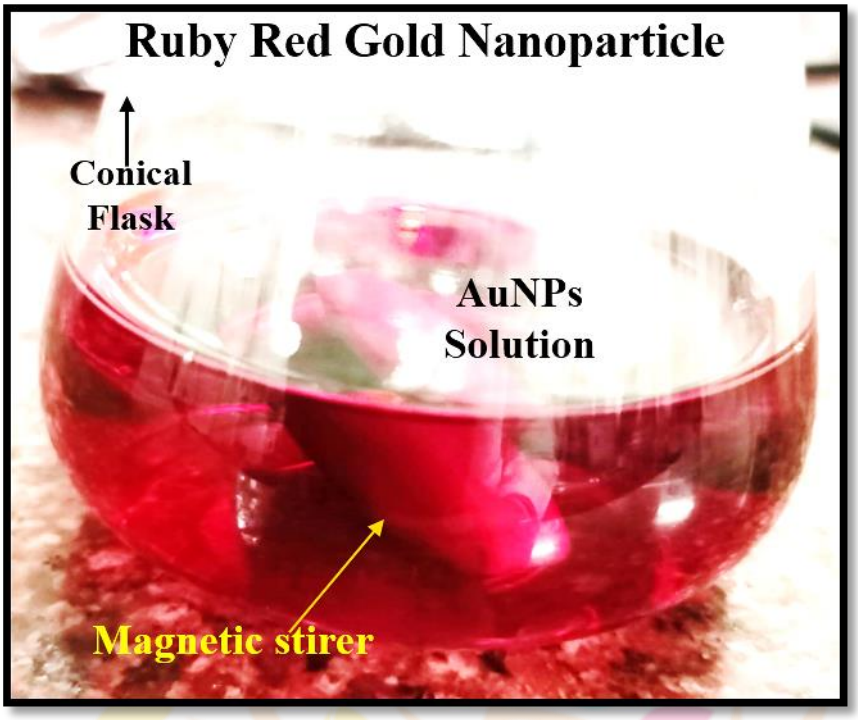

Fig 1. Solution of AuNPs.

2.2.2 UV-Visible Spectrophotometer (UV-Vis Spectrum)

For determining absorption spectra of AuNPs, UV-Vis Spectrophotometer (Lambda-25, Perkin Elmer, USA) was used [28].

2.2.3 Dynamic Light Scattering (DLS)

The hydrodynamic diameter and zeta potential of the AuNPs was determined using dynamic light scattering (MAL 1079370, Version 7.01, Malvern Zetasizer, USA) [29].

2.2.4 X-Ray Diffraction (XRD)

The AuNPs was analyzed following X-ray diffraction (Malvern PAN analytical X'Pert powder) [30].

2.2.5 Scanning Electron Microscopy (SEM)

The morphology of AuNPs was characterized by using scanning electron microscopy (JOEL JSM-IT 300 InTouchScope^{TM}) [31, 10].

3. Results

3.1 UV-Vis spectrum of AuNPs

The UV-Vis spectrum of AuNPs exhibited a characteristic absorption at 524 nm due to surface plasmon resonance (Fig 2).

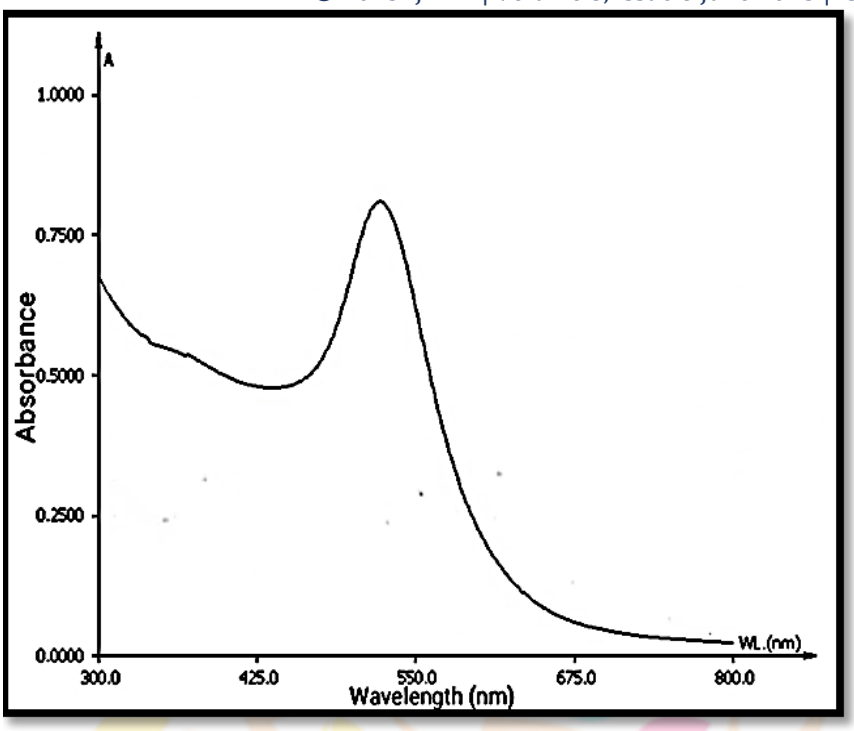

Fig 2. UV-Vis Spectrum of AuNPs.

3.2 DLS

The size and zeta potential of AuNPs were found to be 51 nm (Fig 3) and -20.99 (Fig 4) respectively.

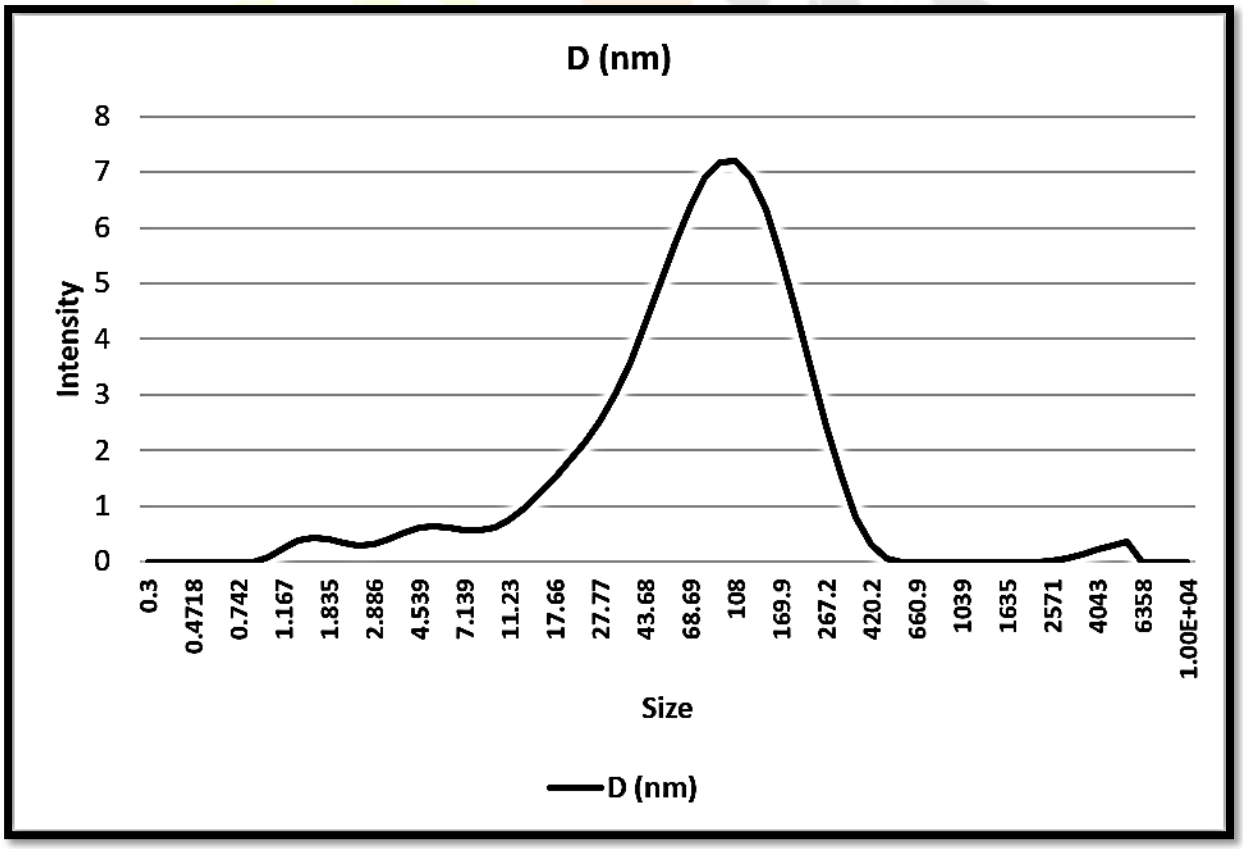

Fig 3. Depicting average size of the AuNPs.

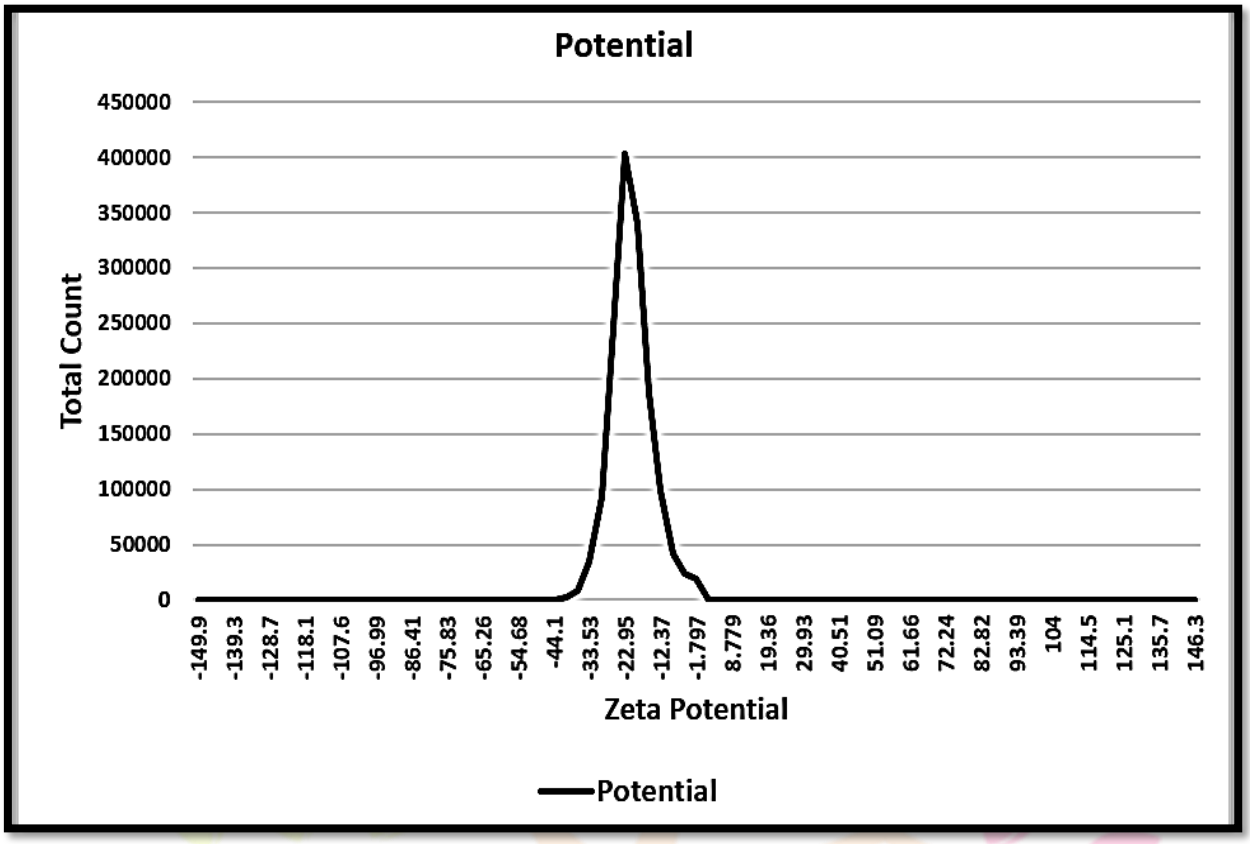

Fig 4. The zeta potential of AuNPs.

3.3 SEM

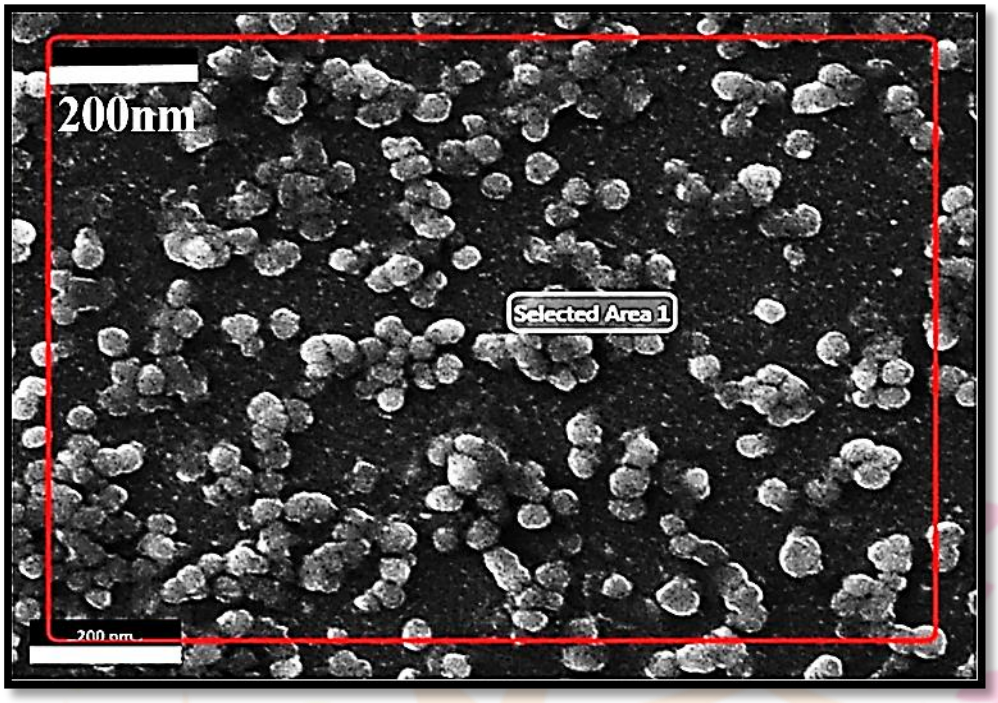

Fig 5. SEM Image of AuNPs.

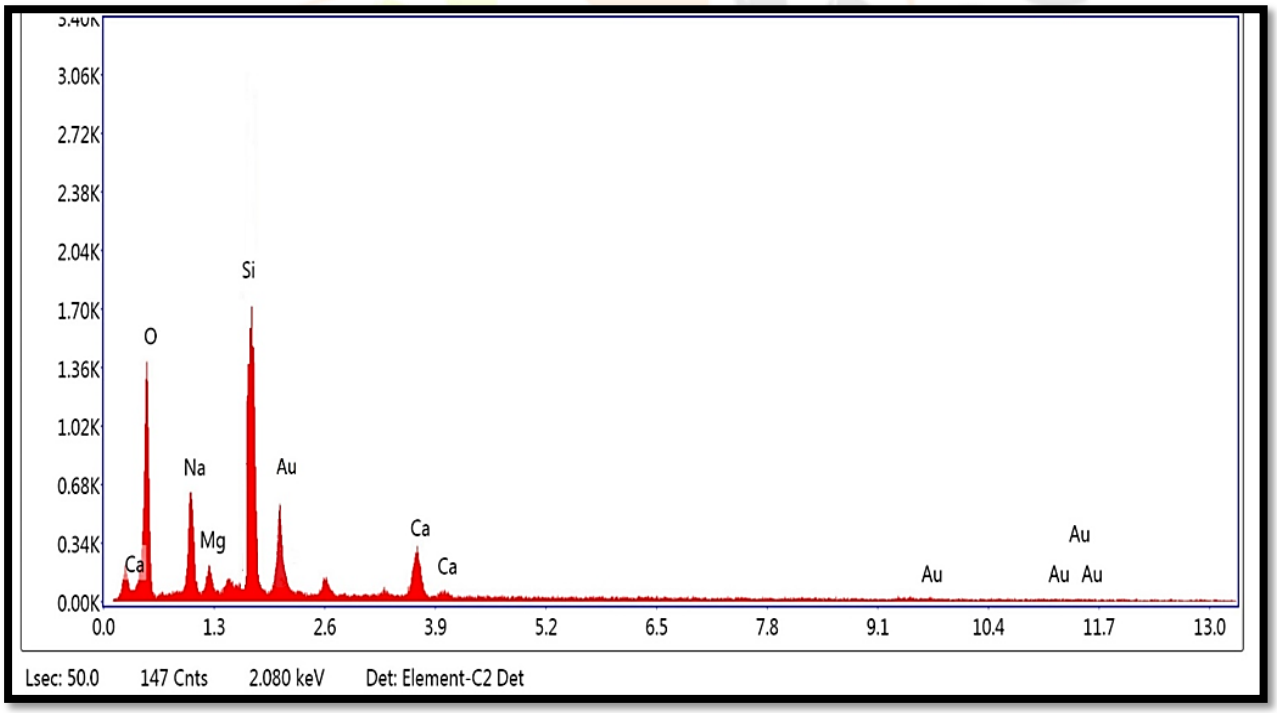

Fig 6. EDX plot of AuNPs.

3.4 XRD

XRD peaks at angle 2 ϴ = 32°, 38°, 44°, 45°, 65°, 77°, 78°; confirmed the crystalline nature of AuNPs.

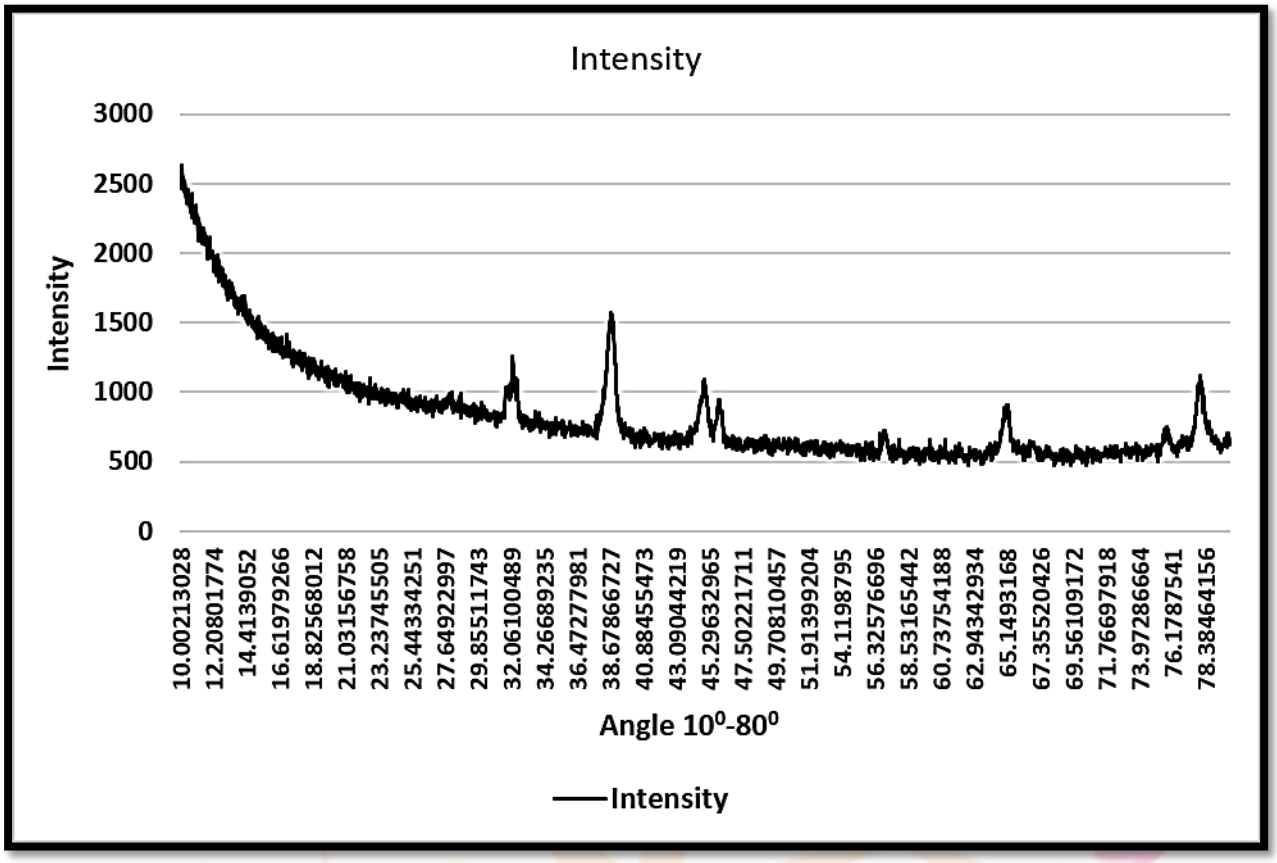

Fig 7. XRD plot Angle 2 ɵ versus Intensity of AuNPs.

3.5 Spectral analysis of paraoxon

Absorption peaks of different concentrations *viz.;* 0.00001 M, 0.00003 M and 0.00005 M of paraoxon were analyzed, and PBS buffer (0.1 M, pH 7.4) was used to set zero of the UV-Vis spectrophotometer. Absorption peak of paraoxon was determined at 400 nm, while, of 4-nitrophenol was obtained at 300 nm, which is a derivative of paraoxon and forms after reaction with water molecule.

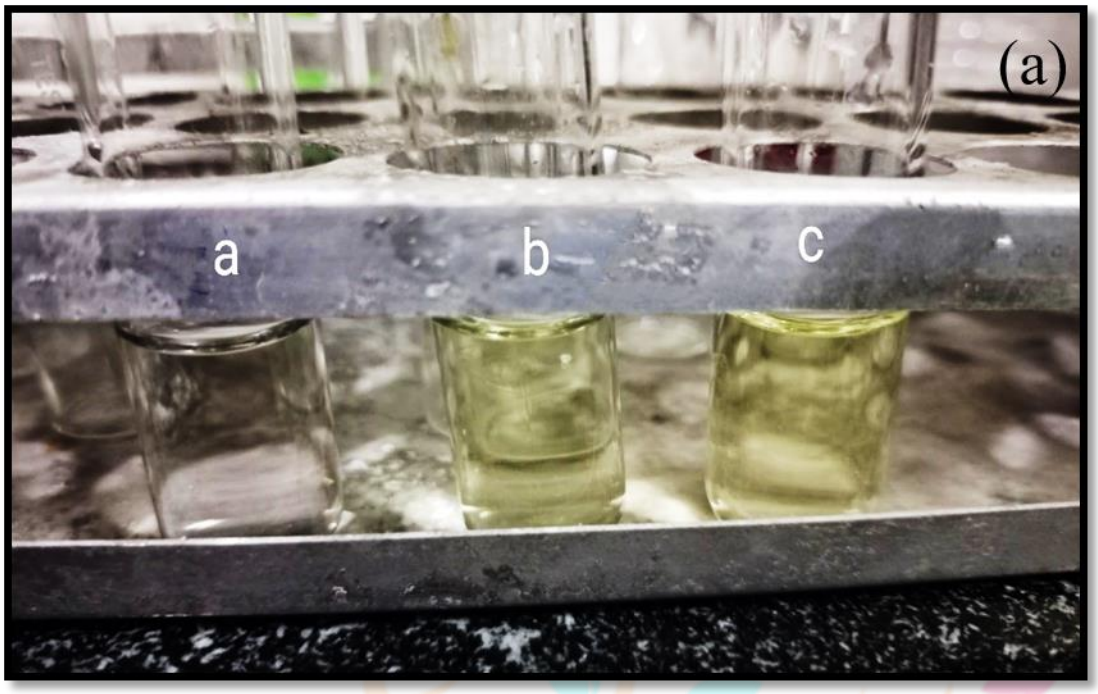

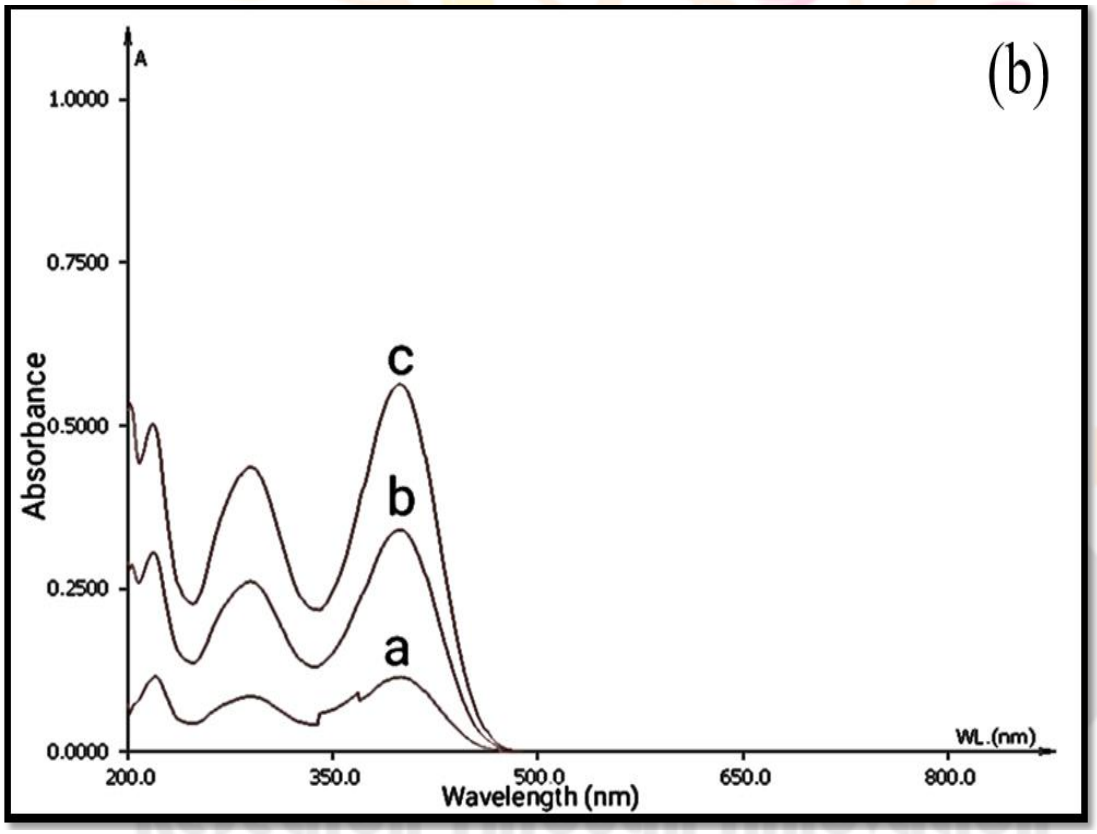

Fig 8. (a) Solutions of PBS buffer (0.1 M, pH 7.4) and paraoxon of different concentrations: 0.00001 M (a), 0.00003 M (b), and 0.00005 M (c) and (b) UV-Vis spectrum of PBS buffer (0.1 M, pH 7.4) and paraoxon of different concentrations: 0.00001 M (a), 0.00003 M (b), and 0.00005 M (c).

3.6 Addition of paraoxon to AuNPs

Different concentrations (0.00001 M, 0.00003 M and 0.00005 M) of paraxon were directly added to the solution of AuNPs. Neither any aggregation nor change in the colour of the solution of AuNPs and paraoxon were observed. In addition, UV-Vis spectra of the solutions were obtained at 524 nm.

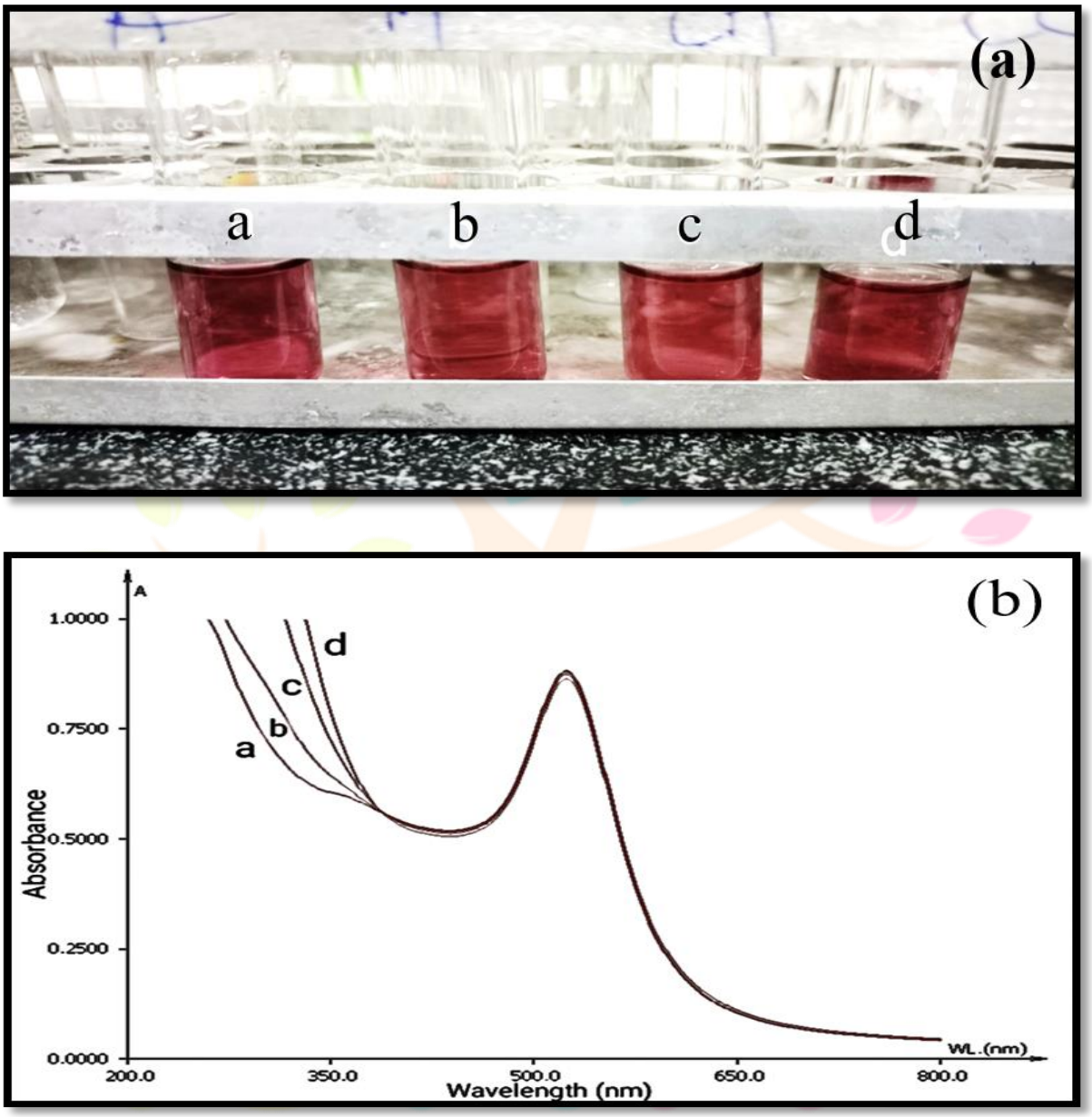

Fig 9. (a). Solutions of AuNPs alone (a), and mixture of AuNPs and different concentrations: 0.00001 M (b), 0.00003 M (c), and 0.00005 M (d) of paraoxon. And (b) UV-Vis spectrum of AuNPs (a), and mixture of AuNPs and different concentrations: 0.00001 M (b), 0.00003 M (c), and 0.00005 M (d) of paraoxon.

3.7 Effect of NaCl on AuNPs

A slight shift in the plasmon peak of the AuNPs was observed after addition of NaCl, more especially after subjection of higher concentrations *i.e*. 0.01 M, 0.03 M and 0.05 M of it. All the plasmon band of NaCl displays a different absorption with respect to the others. Here, PBS buffer (0.1 M, pH 7.4) was used to maintain the pH of the solution.

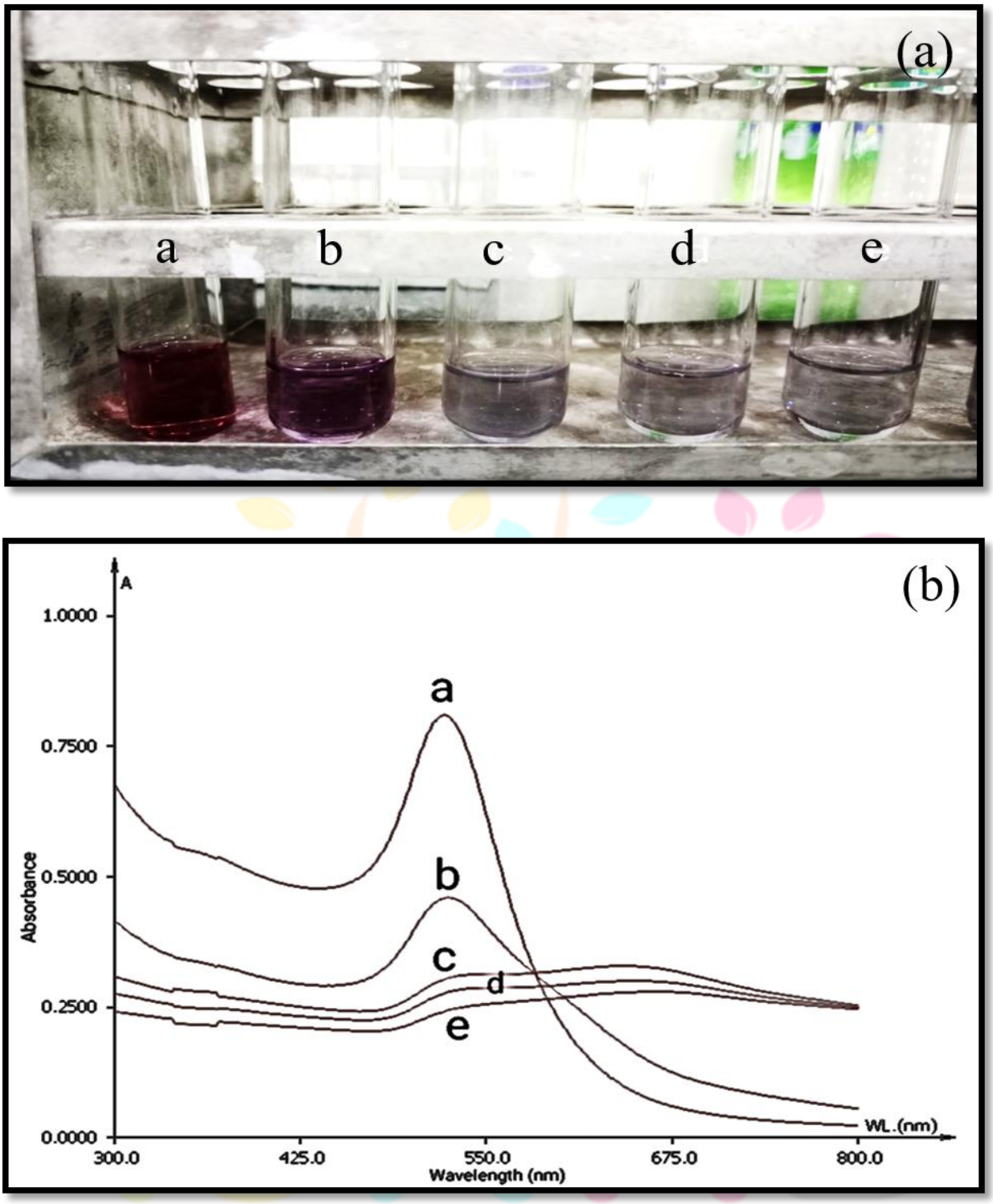

Fig 10. (a). Solutions of AuNPs alone (a), AuNPs + PBS buffer (0.1 M, pH 7.4) (b), and AuNPs + PBS buffer (0.1 M, pH 7.4) + NaCl of 0.01 M (c), 0.03 M (d), and 0.05 M (e). And (b) UV-Vis spectrum of AuNPs (a), AuNPs + PBS buffer (0.1 M, pH 7.4) (b), and AuNPs + PBS buffer (0.1 M, pH 7.4) + NaCl of 0.01 M (c), 0.03 M (d), and 0.05 M (e).

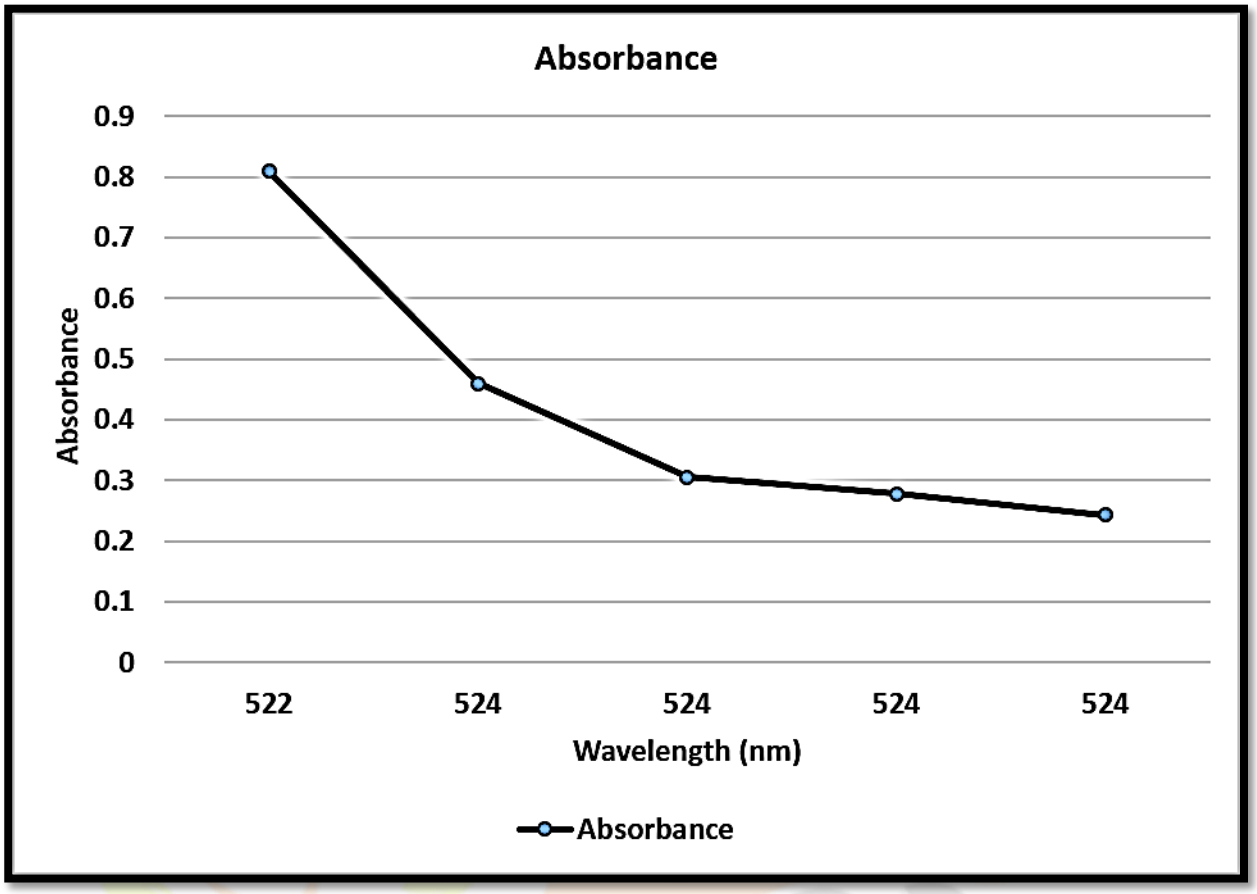

Fig 10 (C). Plot of the wavelength and absorbance of AuNPs and PBS buffer (0.1 M, pH 7.4) versus NaCl concentrations.

3.8 AuNPs and NaCl with different concentrations of paraoxon

Solution of AuNPs, NaCl (0.05M) and PBS buffer (0.1 M, pH 7.4) showed an immediate change in color when paraoxon of different concentrations (0.00001 M, 0.00003 M, and 0.00005 M) was added to it. The absorption spectrum of the samples before and after addition of paraoxon revealed an increase in the peaks at both the wavelengths *i.e*. 524 nm and 400 nm (Fig 11 B).

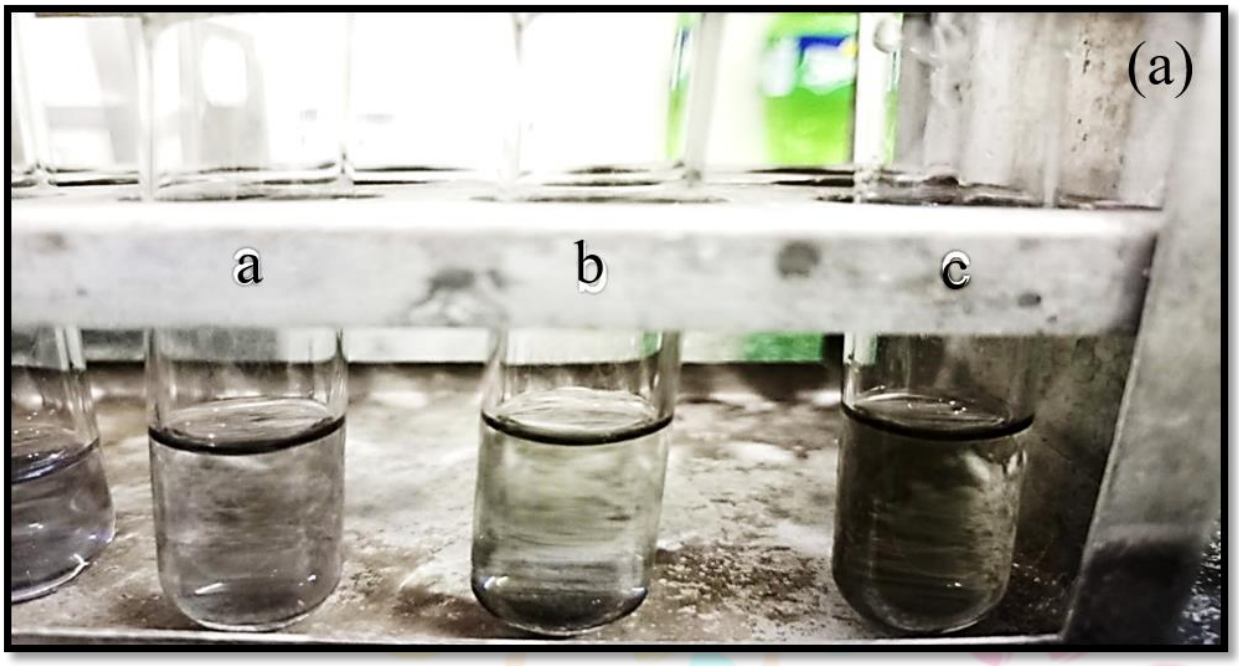

Fig 11 (A).

Solutions of AuNPs + PBS buffer (0.1 M, pH 7.4) + NaCl (0.05 M) and having different concentrations; 0.00001 M (a), 0.00003 M (b), and 0.00005 M (c) of paraoxon.

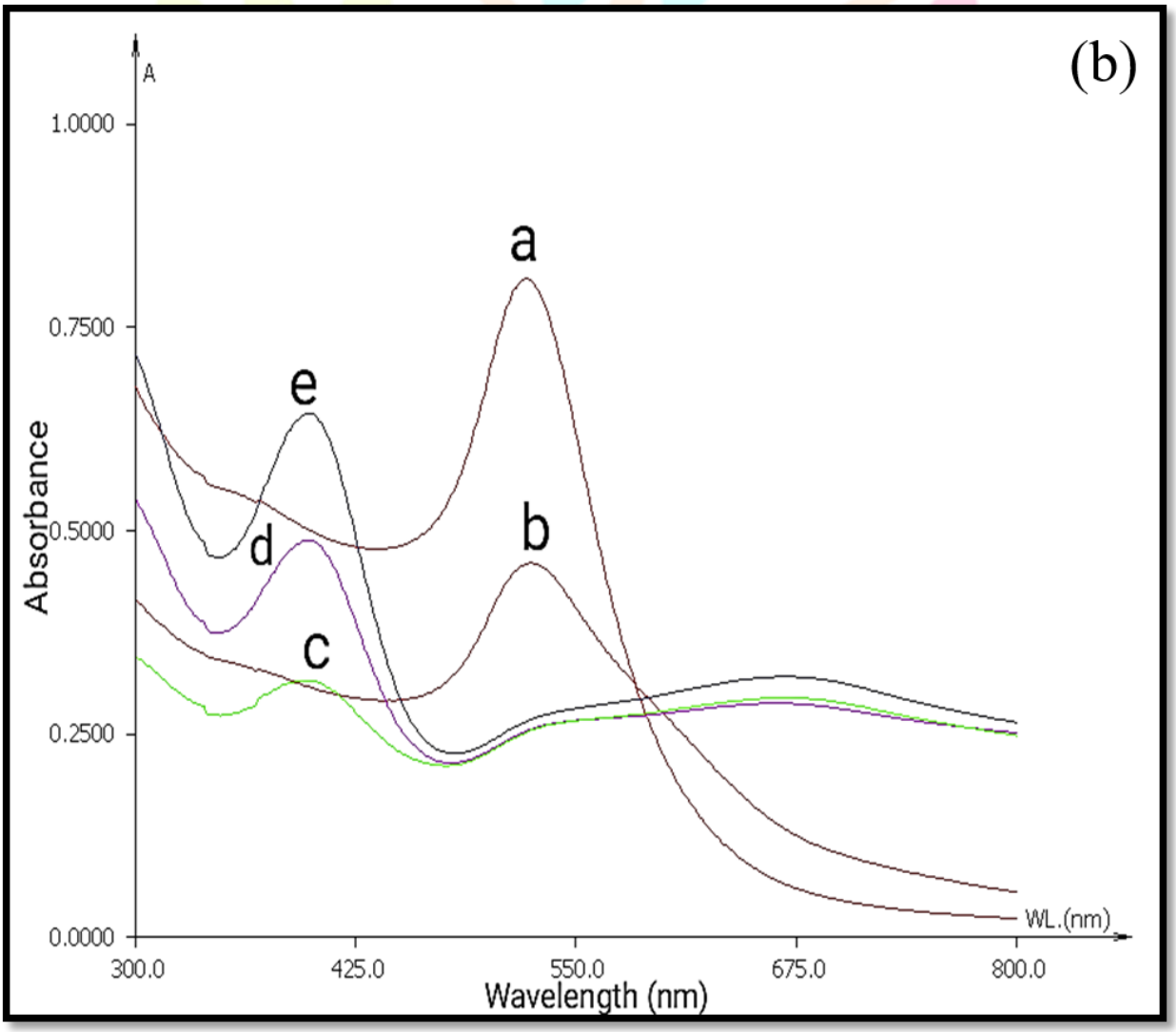

Fig 11 (B). UV-vis spectrum of AuNPs (a), AuNPs + PBS buffer (0.1 M, pH 7.4) + NaCl (0.05 M) (b), and AuNPs + PBS buffer (0.1 M, pH 7.4) + NaCl (0.05 M) + different concentrations; 0.00001 M (c), 0.00003 M (d), and 0.00005 M (e) of paraoxon.

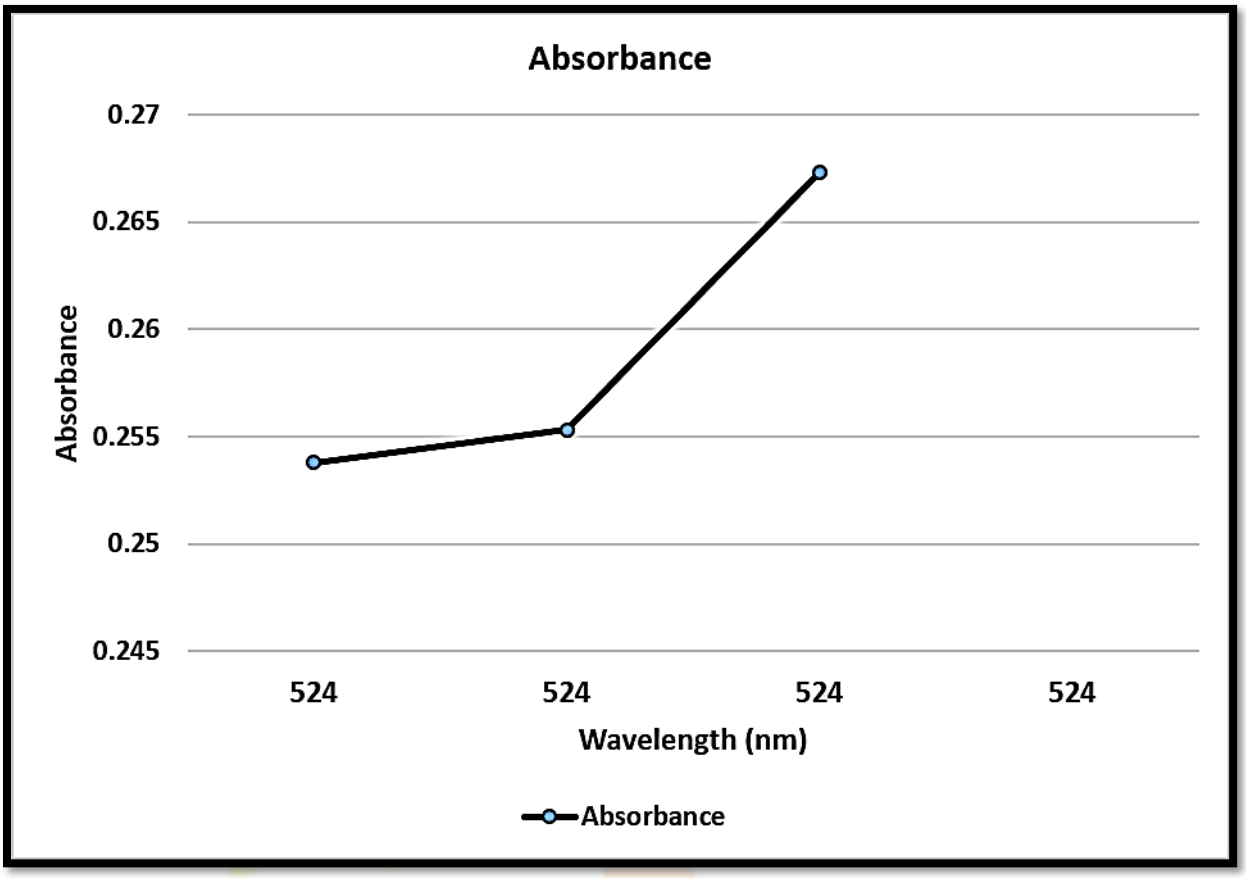

Fig 11 (C). Plot of the wavelength and absorbance of AuNPs + PBS buffer (0.1 M, pH 7.4) + NaCl (0.05 M) versus paraoxon of different concentrations at 524 nm.

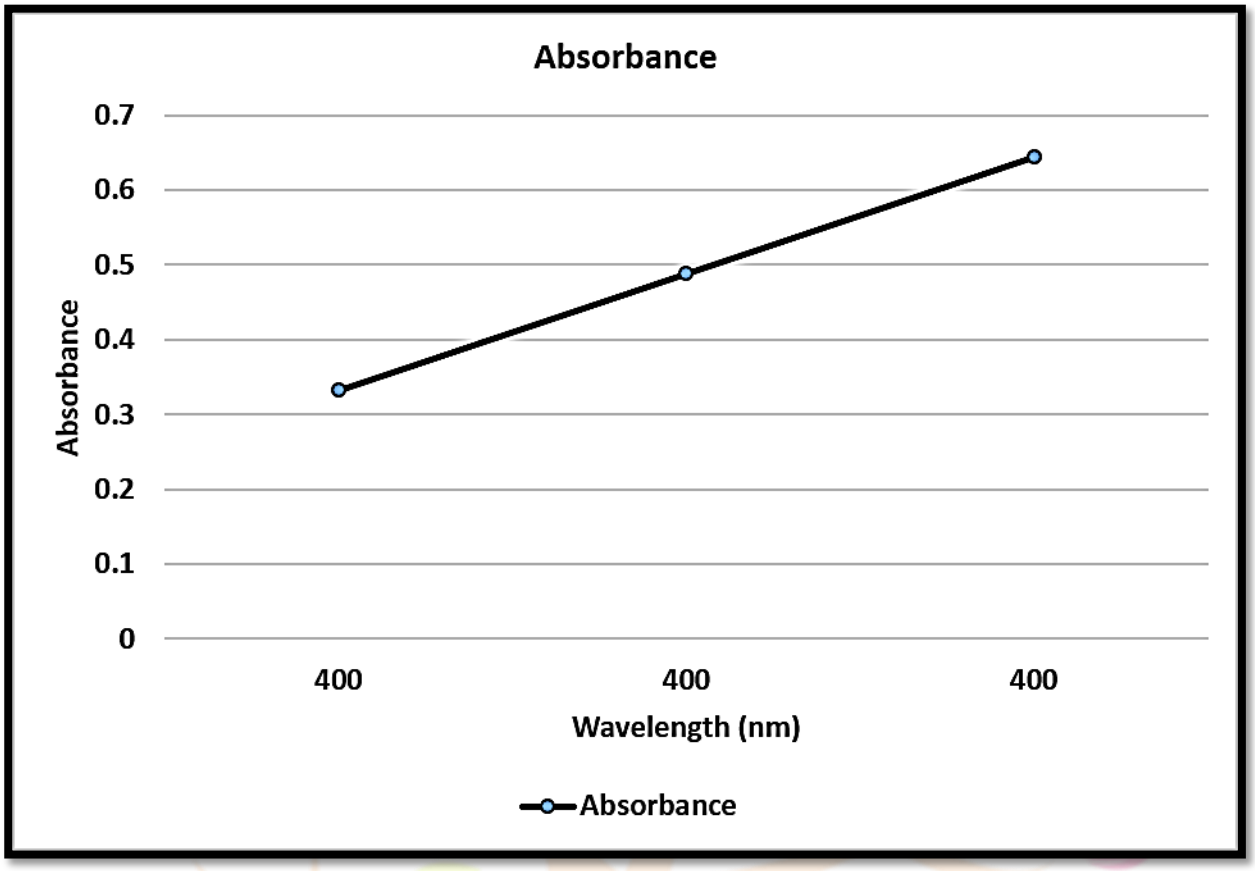

Fig 11 (D). Plot of the wavelength and absorbance of AuNPs + PBS buffer (0.1 M, pH 7.4) + NaCl (0.05 M) versus paraoxon of different concentrations at 400 nm.

3.9 Overall experiment

On the basis of pilot experiments, we finalized a more suited concentration of NaCl as 0.05 M for its addition with the mixture of AuNPs and PBS buffer (0.1 M, pH 7.4). Later, in this mixture, different concentrations; 0.00001 M, 0.00003 M, and 0.00005 M of paraoxon was added to see any change in the color of the sample. Change in color from red to blue and then blue to black indicates the sensitivity of this system towards detection of even trace concentration of paraoxon in an aqueous solution. The absorption spectra of the samples before and after addition of paraoxon were recorded at a wavelengths of 524 nm and 400 nm.

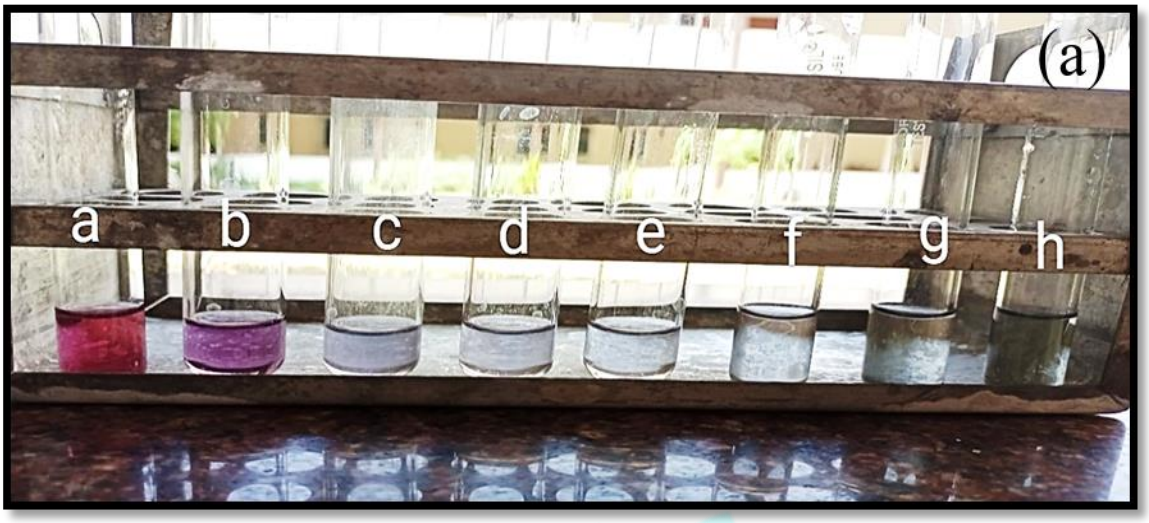

Fig 12. (A) Depicting solutions of AuNPs (a), AuNPs + PBS buffer (0.1 M, pH 7.4) (b), AuNPs + PBS buffer (0.1 M, pH 7.4) + NaCl of different concentrations; 0.01 M (c), 0.03 M (d), and 0.05 M (e), and AuNPs + PBS buffer (0.1 M, pH 7.4) + NaCl (0.05 M) + paraoxon of different concentrations; 0.00001 M (f), 0.00003 M (g), and 0.00005 M (h).

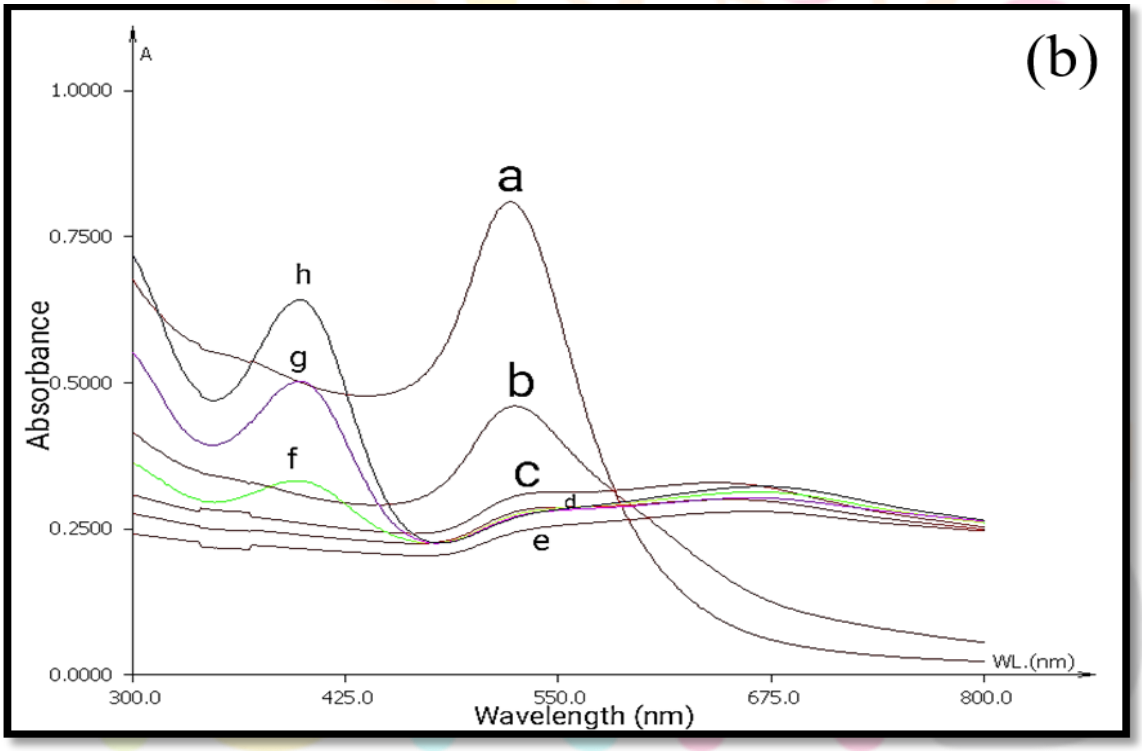

Fig 12. (B) UV-Vis spectrum of AuNPs (a), AuNPs + PBS buffer (0.1 M, pH 7.4) (b), AuNPs + PBS buffer (0.1 M, pH 7.4) + NaCl of different concentrations; 0.01 M (c), 0.03 M (d), and 0.05 M (e) and AuNPs + PBS buffer (0.1 M, pH 7.4) + NaCl (0.05 M) + paraoxon of different concentrations; 0.00001 M (f), 0.00003 M (g), and 0.00005 M (h).

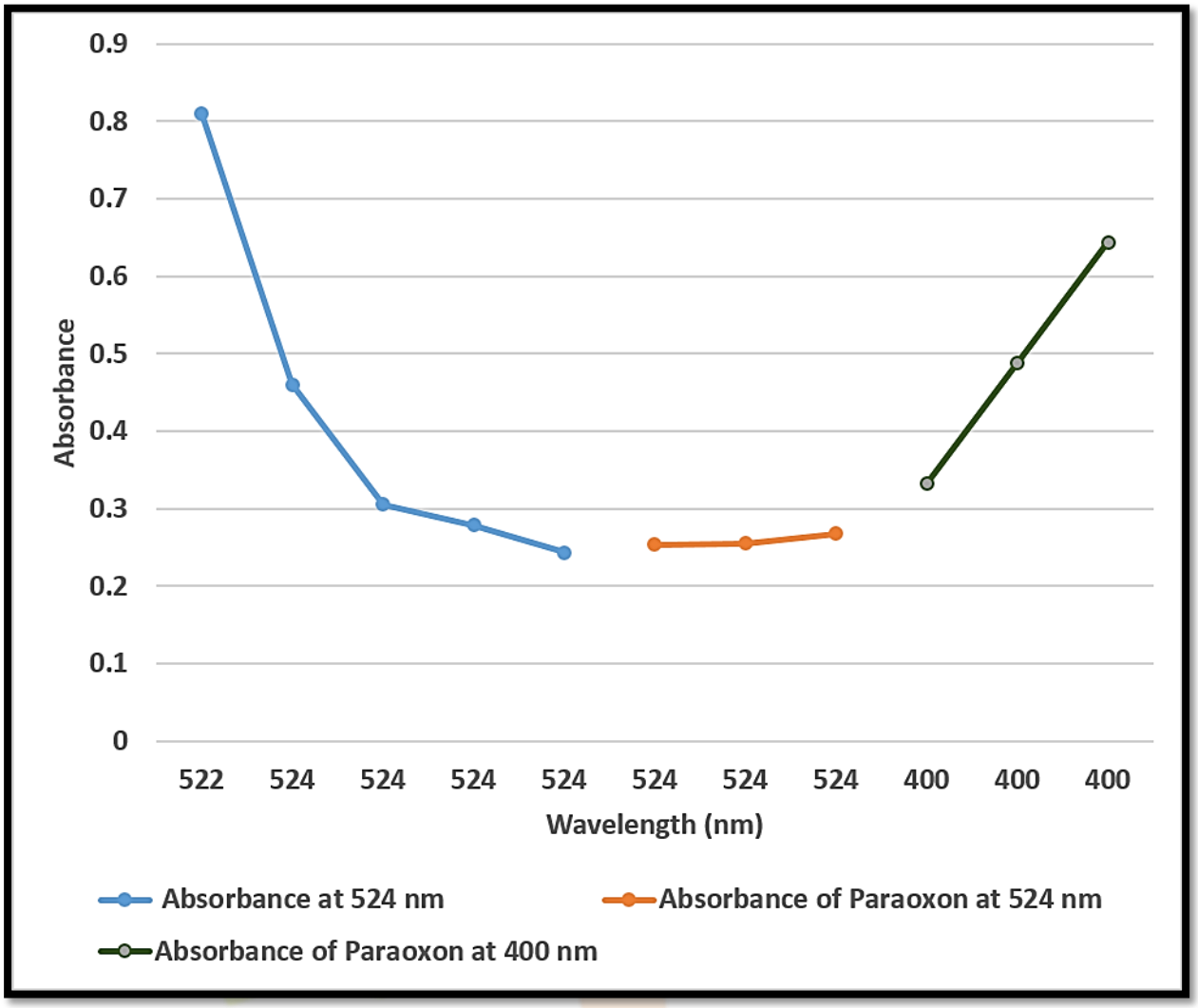

Fig 12. (C) Plot of the wavelength and absorbance of AuNPs + PBS buffer (0.1 M, pH 7.4) versus NaCl at 524 nm and AuNPs + PBS buffer (0.1 M, pH 7.4) + NaCl (0.05 M) versus paraoxon concentrations; 0.00001 M, 0.00003 M, and 0.00005 M at 524 nm and 400 nm.

Analysis of ground water

Performance of the designed system in a complex environment was studied using ground water as a sample. Quality parameters of the ground water sample used in the study were given below;

Parameters	***Quantity***
pH at 25 ◦C	8.01
Fluoride	2.30 ppm
Total alkalinity (as CaCO3)	217 ppm
Total hardness (as CaCO3)	178 ppm
Conductivity at 25 ◦C	565 µmhos/cm
Organic carbon	< 0.5 ppm
Total Dissolved Solids	384 ppm
Calcium (as Ca)	36 ppm

Magnesium (as Mg)	22 ppm
Sulfate (as SO4)	25 ppm
Chloride (as Cl−1)	13 ppm
Phosphate (as PO−3 4)	<0.02 ppm
Iron (as Fe)	<0.001 ppm
Nitrate (as NO-3)	38.9 ppm
Turbidity (as NTU)	0.2 NTU
Silica (as SiO2)	47.4 ppm
Manganese	<0.001 ppm

Collected round water was initially spiked with the paraoxon. Thereafter, colorimetric detection was done after addition of quite lower concentration *i.e.* 0.0000015 M of paraoxon. Appearance of a broad plasmon absorption peak at higher wavelength indicated the presence of paraoxon in the sample. Change in color of the paraoxon spiked sample was clearly distinguishable.

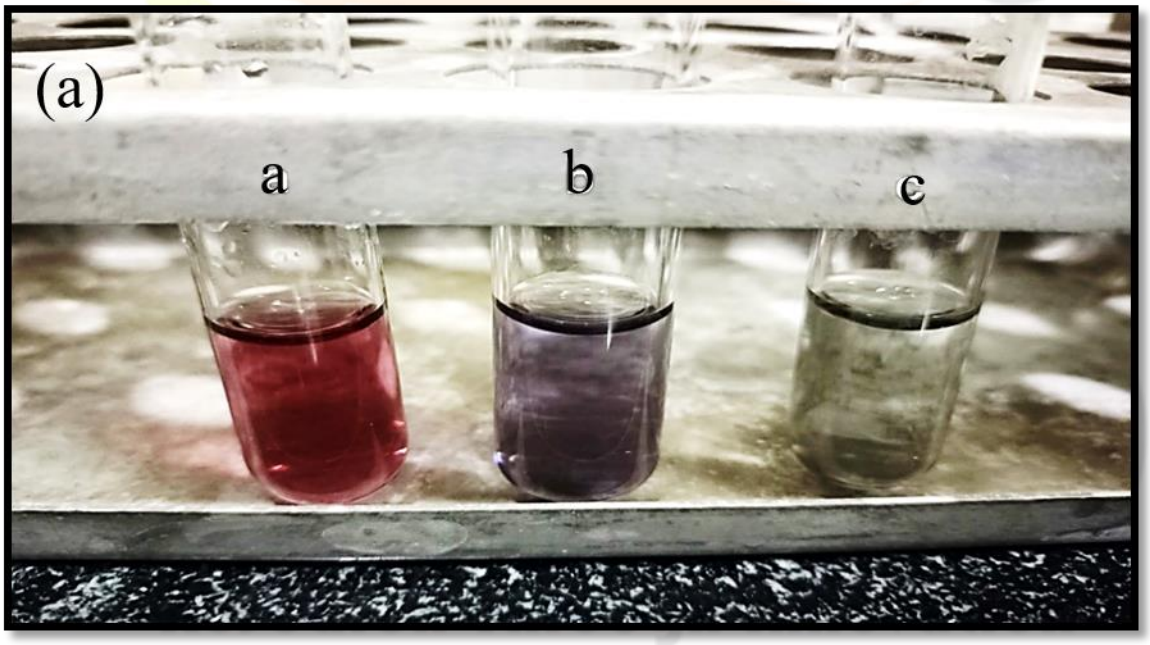

Fig 13 (A). Showing solutions of AuNPs (a), AuNPs + PBS buffer (0.1 M, pH 7.4) + NaCl (0.05 M) (b), and AuNPs + PBS buffer (0.1 M, pH 7.4) + NaCl (0.05 M) + ground water sample spiked with paraoxon (0.0000015 M) (c).

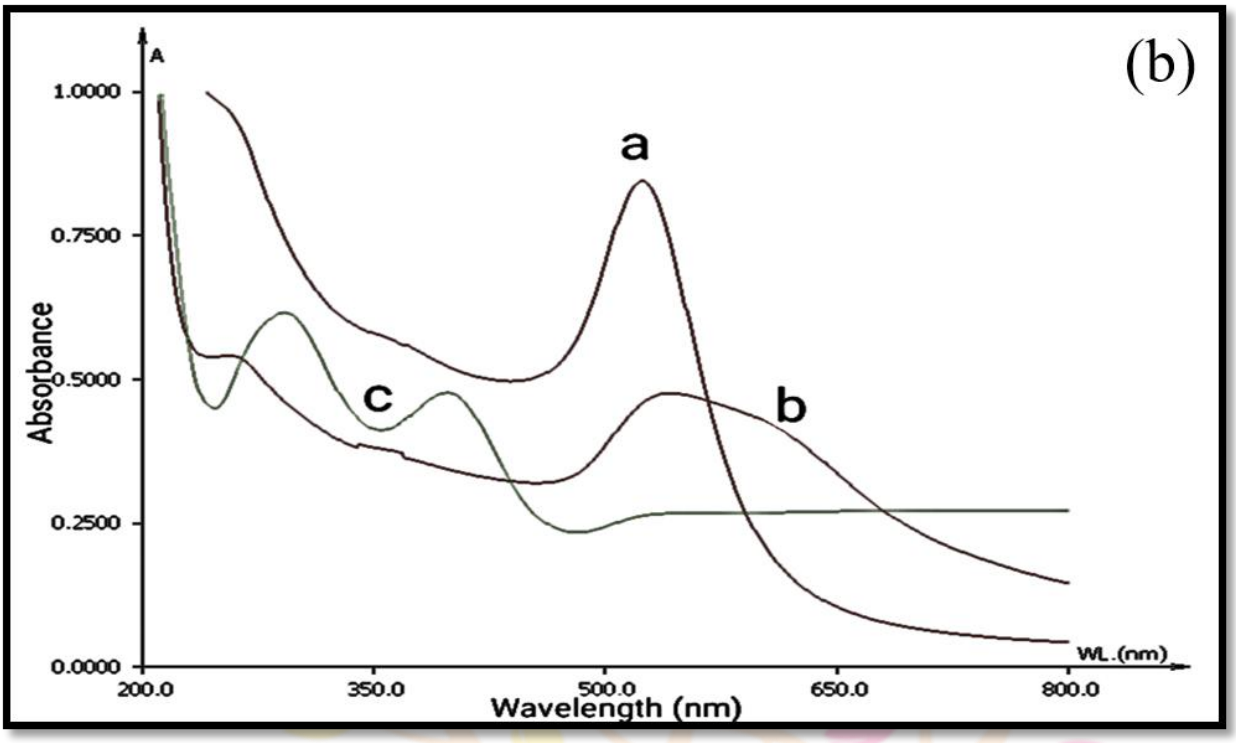

Fig 13 (B). UV-Vis spectrum of AuNPs (a), AuNPs + PBS buffer (0.1 M, pH 7.4) + NaCl (0.05 M) (b), and AuNPs + PBS buffer (0.1 M, pH 7.4) + NaCl (0.05 M) + ground water sample spiked with paraoxon (0.0000015 M) (c).

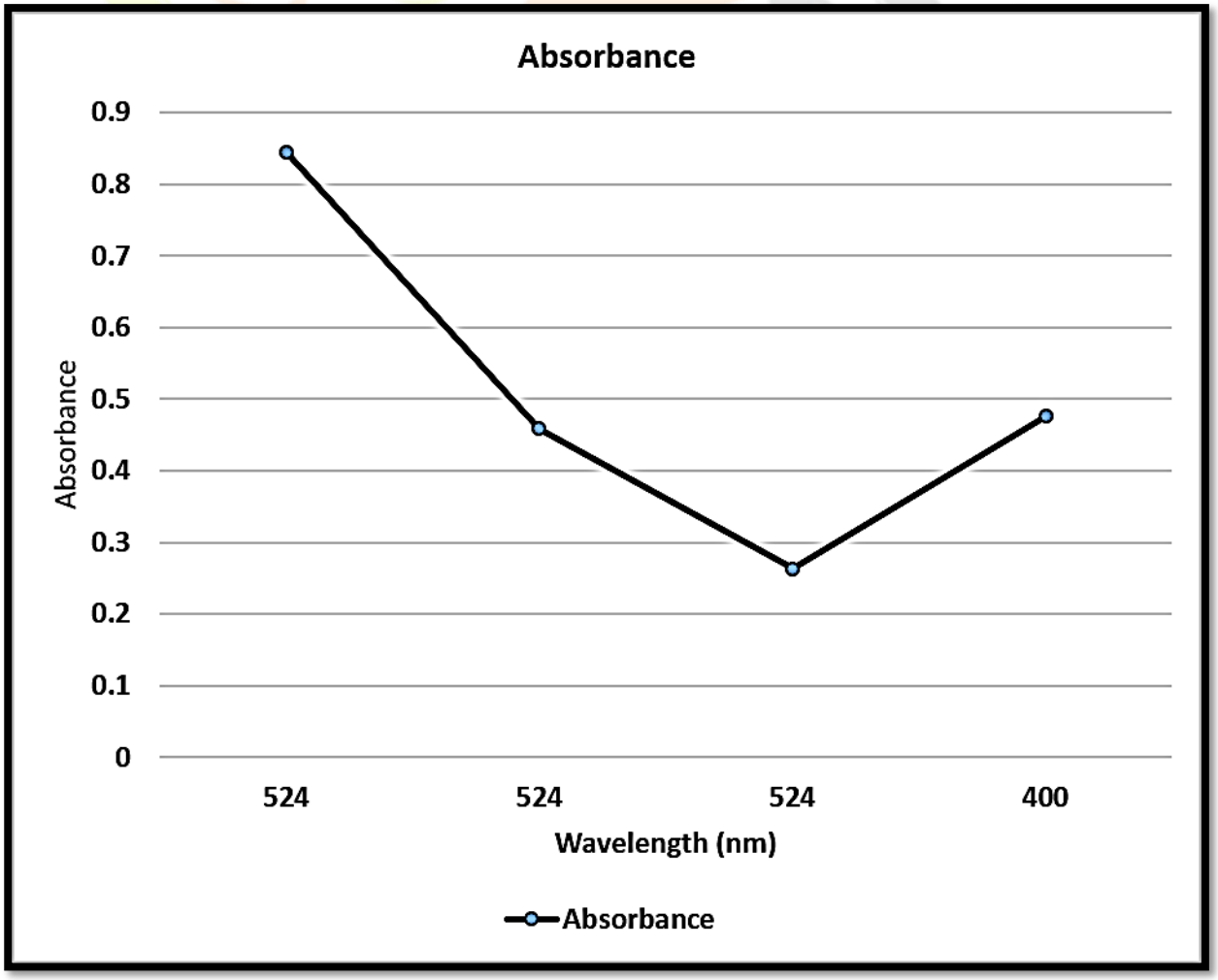

Fig 13 (C). Plot of the wavelength and absorbance of AuNPs + PBS buffer (0.1 M, pH 7.4) + NaCl (0.05 M) versus ground water sample at 524 nm and 400 nm.

Discussions

Nanotechnology has many advantages and is a superb technology for producing NPs which have huge variety of applications. Among them, AuNPs contain unique functional properties and easy to synthesize. Gold NPs with a mean diameter of 1 nm–100 nm has been synthesized via means of reduction of $HAuCl_4.3H_2O$ with trisodium citrate and sodium borohydride. Absorption and scattering properties of AuNPs can be tuned through controlling the particle size, shape, and the local refractive index close to the particle surface. Smaller nanospheres primarily absorb light and show peaks near 520 nm, while larger spheres exhibit increased scattering and have peaks that broaden significantly and shift towards longer wavelengths (called as red-shifting). Optical properties of AuNPs also depend on the refractive index near the NPs surface, this means that the location of extinction peaks of NPs will shift to shorter wavelengths (blue-shift) if the particles are transferred from water to air, or shift to longer wavelengths if the particles are transferred to oil [3, 32].

During the synthesis of NPs, the citrate ions act both as reducing and capping agents. Therefore, the surface of the AuNPs is coated by citrate ions attached by electrostatic and non-specific interactions. The AuNPs are thus stabilized by charge repulsion. The UV-vis spectrum showed the characteristic peak of small spherical AuNPs at 524 nm. The most common method for production of AuNPs is based on citrate reduction and stabilization, known as Turkevich method [13]. With an increase in the ionic strength and concentration of NaCl, the interparticle distance between the AuNPs was effectively reduced. This modification in the plasmon band reveals appearance of large aggregates of NPs. Such aggregation is mediated by the shielding effect of the repulsive electrostatic interactions between the citrate ions coating the NPs and sodium ions available in the solution.

The absorption peak of paraoxon lies in the range of 380 nm – 450 nm, while absorption peak of 4 nitrophenol, a derivative of paraoxon, was obtained in between 300 nm - 315 nm [33]. In agreement, in the current study also absorption peaks of 4-nitrophenol and paraxon were obtained at 300 nm and 400 nm respectively as shown in fig 8 (B). Here, PBS buffer (0.1 M, pH 7.4) was used to maintain the pH.

Upon direct addition of different concentrations (0.00001 M, 0.00003 M and 0.00005 M) of paraxon into the solution of AuNPs, neither any aggregation nor change in the color of the obtained mixture was noticed as shown in fig 9 (A). In addition, UV-Vis spectrum of above solutions was also obtained at 524 nm, which revealed that the paraoxon did not pose any change in the surface properties of AuNPs as shown in fig 9 (B).

Increase in the concentration of NaCl reduced the interparticle distance between the AuNPs. Higher concentrations of NaCl has been seen to irreversibly control the aggregation of AuNPs as shown in fig 10 (A). Modification/ slight shifting in the plasmon peak of the AuNPs was observed in response to higher concentrations; 0.01 M, 0.03 M, and 0.05 M of NaCl as shown in fig 10 (B). All the plasmon bands of NaCl displayed a different absorption with respect

to the others. This modification in the plasmon band, with a broad peak ascribes the appearance of large aggregates of AuNPs. Such aggregation is mediated by the shielding effect of the repulsive electrostatic interactions of the citrate ions coating the AuNPs by the sodium ions in solution [14].

Visual detection of the presence of paraoxon is possible when there was a change in the color of the solution due to adsorption of this pesticides on AuNPs which is enhanced/ mediated by the NaCl [34]. In the current approach, a change in the color change of citrate-capped AuNPs in presence of NaCl (0.05 M) and PBS buffer (0.1 M, pH 7.4) and in response to addition of different concentrations (0.00001 M, 0.00003 M and 0.00005 M) of paraoxon from red to blue and then blue to clear black color has been noted as shown in fig 11 (A). Increased aggregation of AuNPs may probably be the reason for paraoxon mediated change in color of the solution. The AuNPs associated colorimetric detection is an effective technique for the determination of paraoxon because of their higher molar extinction coefficient. Presence of this analyte induces changes in the color and SPR wavelength of AuNPs and also results in either aggregation of AuNPs or disassembly of aggregates of AuNPs.

This method was successfully applied to detect presence of paraoxon in the fruit juices, water, soil, *etc*., which approves that we have succeeded in designing a portable system for the detection of paraoxon which was based on the aggregation of citrate caped AuNPs. However, modification in the small molecules available on the surface of AuNPs can possibly improve their selectivity and sensitivity of detection. Following above technique, we can also identify the presence of 4-nitrophenol. The detection of 4-nitrophenol was not affected by the presence of paraoxon as they will produce two different absorption peaks. The 4-nitrophenol and paraoxon will produce their specific absorption peaks at 300 nm and 400 nm respectively as shown in fig 8 (A).

Performance of the developed system in a complex environment was studied using ground water as a sample. Colorimetric detection was done after addition of quite a low concentration 0.0000015 M of paraoxon into the ground water. The appearance of a broad plasmon absorption peak at higher wavelength indicated the presence of paraoxon in the sample. The change in color of the sample spiked with paraoxon was clearly distinguishable as shown in fig 13 (A).

The technique proposed here is a straight forward method and there is no need of sample preparation. The reaction happens within seconds and the change in color of the sample is very clear/ distinct. The technique suggests great potential for onsite monitoring of pesticide. The technique is also applicable as a qualitative method for the evaluation of performance of various household water filters, which claim removal of pesticide.

Conclusions

In this study, synthesis and characterization of AuNPs, and detection of paraoxon, a lethal pesticide, with add of NaCl has been performed. Gold NPs treated with NaCl (0.05 M) has been found to be an effective system for the visual detection of paraoxon. The adsorbed citrate layer on AuNPs interacts with NaCl, which further interacts with paraoxon. Response of this reaction is observable as a rapid change in the color of the mixture. The performance of

AuNPs at different concentrations of NaCl has also been studied. Experiments with ground water sample showed the effectiveness of the detection system. This AuNPs based biosensors can be used as an aid for onsite and real time detection of not only paraoxon but also of several other pesticides and insecticides of similar structural properties. The unique properties of AuNP suggest its broad applications. The wide range of surface functionality and outstanding physical properties of AuNPs make this system important for sensing applications. Gold NPs have multiple attributes which make them potent tools for the use in bionanotechnology.

Acknowledgements

The authors acknowledge the financial support provided by Fund for Improvement of S&T Infrastructure in Universities and Higher Educational Institutions (FIST) Program, Department of Science and Technology (DST), School of Studies in Biotechnology and School of Studies in Chemistry, Pt. Ravishankar Shukla University, Raipur 492 010, Chhattisgarh, India for conducting this research work.

References

[1] Khan I, Saeed K and Khan I (2017) Nanoparticles: properties, applications and toxicities. Arab J Chem 12, 908–931. https://doi.org/10.1016/j.arabjc.2017.05.011

[2] Tayo L L (2017) Stimuli-responsive nanocarriers for intracellular delivery. Biophys Rev 9, 931–940. https://doi.org/10.1007/s12551-017-0341-z

[3] Ramalingam V (2019) Multifunctionality of gold nanoparticles: plausible and convincing properties. Adv Colloid Int Sci 271, 101989. https://doi.org/10.1016/j.cis.2019. 101989

[4] Khan T, Ullah N, Khan M A, Mashwani Z R and Nadhman A (2019) Plant based gold nanoparticles: a comprehensive review of the decade-long research on synthesis, mechanistic aspects and diverse applications. Adv Colloid Int Sci 272, 102017. https://doi.org/10.1016/j.cis.2019.102017

[5] O Neal D P, Hirsch L R, Halas N J, Payne J D and West J L (2004) Photothermal tumor ablation in mice using near infrared-absorbing nanoparticles. Cancer Lett 209, 171–176. https://doi.org/10.1016/j.canlet.2004.02.004

[6] Chen H, Kou X, Yang Z, Ni W and Wang J (2008) Shape and size dependent refractive index sensitivity of gold nanoparticles. Langmuir 24, 5233–5237. https://doi.org/10.1021/la800305j

[7] Li S, Zhang L, Wang T, Li L, Wang C and Su Z (2015) The facile synthesis of hollow Au nanoflowers for synergistic chemo-photothermal cancer therapy. Chem Commun 51, 14338–14341. https://doi.org/10.1039/C5CC05676D

[8] Xiao T, Huang J, Wang D, Meng T and Yang X (2019) Au and Au Based nanomaterials: synthesis and recent progress in electrochemical sensor applications. Talanta 206, 120210. https://doi.org/10.1016/j.talanta.2019.12 0210

[9] Faraday M (1857) Experimental relations of gold (and other metals) to light. Philos Trans R Soc 147, 145–181. https://doi.org/10.1080/14786445708642410

[10] Khanna P, Kaur A and Goyal D (2019) Algae-based metallic nanoparticles: synthesis, characterization and applications. J Microbiol Methods 163, 105656. https://doi.org/10.1016/j.mimet.2019.105656

[11] Chen J, Mela P, Moller P and Lensen M C (2009) Microcontact deprinting: a technique to pattern gold nanoparticles. ACS Nano 3, 1451–1456. https://doi.org/10.1021/ nn9002924

[12] Walters G and Parkin P I (2009) The incorporation of noble metal nanoparticles into host matrix thin films: synthesis, characterisation and applications. J Mater Chem 19, 574–590. https://doi.org/10.1039/B809 646E

[13] Turkevich J, Stevenson P C and Hillier J (1951) A study of the nucleation and growth processes in the synthesis of colloidal gold. Dis Fara Soc 11, 55–75. https://doi.org/10.1039/DF9511100055

[14] Frens G (1973) Controlled nucleation for the regulation of the particle size in monodisperse gold suspensions. Nat Phys Sci 241, 20–22. https://doi.org/10.1038/10. 1038/physci241020a0

[15] Ji X, Song X, Li J, Bai Y, Yang W and Peng X (2007) Size control of gold nanocrystals in citrate reduction: the third role of citrate. J Am Chem Soc 129, 13939–13948. https://doi.org/10.1021/ja074447k

[16] Jimenez I O, Romero F M, Bastus N G and Puntes V (2010) Small gold nanoparticles synthesized with sodium citrate and heavy water: insights into the reaction mechanism. J Phys Chem C 114, 1800–1804. https://doi.org/10.1021/jp9091305

[17] Thuy P T, Van Geluwe S, Nguyen V A and Van der Bruggen B (2012) Current pesticide practices and environmental issues in Vietnam: management challenges for sustainable use of pesticides for tropical crops in (South-East) Asia to avoid environmental pollution. J Mater Cycles Waste Manag 14, 379–387. https://doi.org/10.1007/s10163-012-0081-x

[18] Marican A and Duran-Lara E F (2018) A review on pesticide removal through different processes. Environ Sci Pollut Res 25, 2051–2064. https://doi.org/10.1007/s11356-017-0796-2

[19] Gilden R C, Huffling K and Sattler B (2010) Pesticides and health risks. J Obstet Gynecol Neonatal Nurs 39, 103–210. https://doi.org/10.1111/j.1552-6909.2009.01092.x

[20] Gorell J M, Johnson C, Rybicki B, Peterson E and Richardson R (1998) The risk of Parkinson's disease with exposure to pesticides, farming, well water, and rural living. Neurology 50, 1346–1350. https://doi.org/10.1212/wnl.50.5.1346

[21] Tixier P, Chabrier C and Malezieux E (2007) Pesticide residues in heterogeneous plant populations, a model-based approach applied to nematicides in banana (*Musa* spp.). J Agric Food Chem 55, 2504–2508. https://doi.org/10.1021/jf062710f

[22] Barra R, Vighi M, Maffioli G, Di Guardo A and Ferrario P (2000) Coupling soil fug model and GIS for predicting pesticide pollution of surface water at watershed level. Environ Sci Technol 34, 4425–4433. https://doi.org/10.1021/es000986c

[23] Ko E, Choi M and Shin S (2020) Bottom-line mechanism of organochlorine pesticides on mitochondria dysfunction linked with type 2 diabetes. J Hazard Mater 393, 122400. https://doi.org/10.1016/j.jhazmat.2020.122400

[24] Naous G E-Z, Merhi A, Abboud M I, Mroueh M and Taleb R I (2018) Carcinogenic and neurotoxic risks of acrylamide consumed through caffeinated beverages among the lebanese population. Chemosphere 208, 352–357. https://doi.org/10.1016/j.chemosphere.2018.05.185

[25] Legeay S, Billat P A, Clere N, Nesslany F, Bristeau S and Faure S (2018) Two dechlorinated chlordecone derivatives formed by *in-situ* chemical reduction are devoid of genotoxicity and mutagenicity and have lower proangiogenic properties compared to the parent compound. Environ Sci Pollut Res 25, 14313–14323. https://doi.org/10.1007/s11356-017-8592-6

[26] Kim K H, Kabir E and Jahan S A (2017) Exposure to pesticides and the associated human health effects. Sci Total Environ 575, 525–535. https://doi.org/10.1016/j.scitotenv.2016.09.009

[27] Hayes W J (1975) Toxicology of pesticides. Jr. Pesticides studied in man / Wayland J. Hayes, Jr.

[28] Brown K R, Walter D G and Natan M J (1999) Seeding of colloidal Au nanoparticle solutions. Improved control of particle size and shape. Chem Mater 12, 306–313. https://doi.org/10.1021/cm980065p

[29] Leonov A P, Zheng J, Clogston J D, Stern S T, Patri A K and Wei A (2008) Detoxification of gold nanorods by treatment with polystyrenesulfonate. ACS Nano 2, 2481–2488. https://doi.org/10.1021/nn800466c

[30] Bastus N G, Comenge J and Puntes V (2011) Gold nanoparticles of up to 200nm: size focusing versus Ostwald ripening. Langmuir 27, 11098–11105. https://doi.org/10.1021/la201938u

[31] Leff D V, Ohara P C, Heath J R and Gelbart W M (1995) Thermodynamic control of gold nanocrystal size: experiment and theory. J Phys Chem 99, 7036–7041. https://doi.org/10.1021/j100018a041

[32] Gurav D D, Jia Y A, Ye J and Qian K (2019) Design of plasmonic nanomaterials for diagnostic spectrometry. Nanoscale Adv 1, 459–469. https://doi.org/10.1039/C8NA00319J

[33] Li B, Sun P, Zhen J, Gong W, Zhang Z, Jia W and Pan L (2021) pH controlled UV−vis sensing strategy for indirect, rapid detection of paraoxon based on molecular form conversion. Sens Actuators B Chem 348, 130715. https://doi.org/10.1016/j.snb.2021.130715

[34] Kinattukara P L, Anshup and Thalappil P (2009) Enhanced visual detection of pesticides using gold nanoparticles. J Environ Sci Health part B 44, 697–705. https://doi.org/10.1080/03601230903163814